JACS
JOURNAL OF THE AMERICAN CHEMICAL SOCIETY

ARTICLE

pubs.acs.org/JACS

Molecular Oxygen Adsorption Behaviors on the Rutile TiO_2(110)-1×1 Surface: An in Situ Study with Low-Temperature Scanning Tunneling Microscopy

Shijing Tan, Yongfei Ji, Yan Zhao, Aidi Zhao, Bing Wang,* Jinlong Yang, and J.G. Hou*

Hefei National Laboratory for Physical Sciences at the Microscale, University of Science and Technology of China, Hefei 230026, Anhui, China

ABSTRACT: A knowledge of adsorption behaviors of oxygen on the model system of the reduced rutile TiO_2(110)-1×1 surface is of great importance for an atomistic understanding of many chemical processes. We present a scanning tunneling microcopy (STM) study on the adsorption of molecular oxygen either at the bridge-bonded oxygen vacancies (BBO_V) or at the hydroxyls (OH) on the TiO_2(110)-1×1 surface. Using an in situ O_2 dosing method, we are able to directly verify the exact adsorption sites and the dynamic behaviors of molecular O_2. Our experiments provide direct evidence that an O_2 molecule can intrinsically adsorb at both the BBO_V and the OH sites. It has been identified that, at a low coverage of O_2, the singly adsorbed molecular O_2 at BBO_V can be dissociated through an intermediate state as driven by the STM tip. However, singly adsorbed molecular O_2 at OH can survive from such a tip-induced effect, which implies that the singly adsorbed O_2 at OH is more stable than that at BBO_V. It is interesting to observe that when the BBO_Vs are fully filled with excess O_2 dosing, the adsorbed O_2 molecules at BBO_V tend to be nondissociative even under a higher bias voltage of 2.2 V. Such a nondissociative behavior is most likely attributed to the presence of two or more O_2 molecules simultaneously adsorbed at a BBO_V with a more stable configuration than singly adsorbed molecular O_2 at a BBO_V.

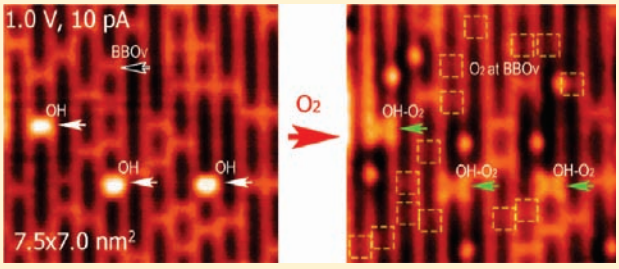

1. INTRODUCTION

The adsorption of molecular oxygen on titanium dioxide has attracted extensive study interests since adsorbed oxygen plays an important role in many surface chemical processes,[1−3] particularly for the low-temperature oxidation reactions in heterogeneous catalysis,[4] as well as in photocatalysis.[5] In general, adsorbed O_2 acts as a scavenger to excess electrons originating from donor-specific sites, such as bridge-bonded oxygen vacancies (BBO_V), hydroxyl groups (OH), and Ti interstitials.[6−15] Scanning tunneling microscopy (STM) has been used to characterize adsorbed molecules on the TiO_2 surface and provide useful information for understanding the chemical processes at the atomic scale. Some recent efforts using STM have been made to understand the adsorption of molecular oxygen on the reduced rutile TiO_2(110)-1×1 surface.[12,16] However, adsorption of molecular oxygen at low temperatures remains a puzzling problem.[7,8,14,17−20] The STM results showed dissociative O_2, either dissociated at BBO_V with one O atom healing the BBO_V and the other O atom leaving at a neighboring 5-fold-coordinated Ti (Ti_{5c}) site as an adatom,[18,20−22] or dissociated directly at Ti_{5c} sites, yielding paired O adatoms which may be caused by Ti interstitials.[7,23] It was reported that the O_2 molecule may also react with the hydroxyl group, yielding HO_2 species.[9,24−26] On the other hand, the photodesorption experiments indicate two states of molecular O_2 at BBO_V.[6] The temperature-programmed desorption (TPD) measurements suggest that up to three O_2 molecules adsorb per BBO_V at 120 K, but a dissociation channel is favored above 150 K.[8] A recent result reports that two O_2 molecules chemisorb per BBO_V and convert to a stable tetra-oxygen as annealed above 200 K,[27] which was predicted by the theoretical results.[28] In photocatalysis, it is reported that the molecular oxygen plays an indispensable role, assisting the charge separation and generating the active species of O_2^-, O_2^{2-}, HO_2, etc.[9,29−31] Such molecular oxygen species on TiO_2 are required to be comprehensively understood at a molecular scale, especially on their actual adsorption sites, in the interaction with the TiO_2 surface, and in the reaction with other adsorbed species.

In this study, we investigated O_2 adsorption on TiO_2(110) surfaces with BBO_V and OH. The adsorption behaviors of molecular O_2 were systematically studied with various coverages of O_2 and different temperatures using STM. The dissociation of O_2 molecules at BBO_V was measured at different temperatures and different O_2 coverages. The dissociation processes are analyzed and simulated using first-principle calculations. The interaction of O_2 with OH is also studied, which shows a behavior different from that of adsorbed O_2 at BBO_V. Our study provides a comprehensive picture of O_2 adsorption and some insights into the role of O_2 as a scavenger to excess electrons in the chemical reactions mediated by TiO_2 surfaces.

Received: November 18, 2010
Published: January 19, 2011

dx.doi.org/10.1021/ja110375n | J. Am. Chem. Soc. 2011, 133, 2002–2009

2. EXPERIMENTAL SECTION

The experiments were conducted in an ultra-high-vacuum low-temperature STM (LT-STM) system (Omicron, base pressure <3 × 10^{-11} mbar). The reduced rutile TiO_2(110)-1×1 surface was prepared by repeated cycles of 1000 eV of Ar^+ sputtering and annealing to 900 K with a Ta-foil heater behind the sample. The clean TiO_2(110)-1×1 surface was then transferred to the cryostat of the microscope, which had been precooled to 80 or 5.2 K. The STM measurements were performed mostly at 80 and 5.2 K, at which the microscope has good performance in thermal stability. Variable-temperature experiments have also been performed by warming the sample from 80 to 130 K. The O_2 (99.999%) dosing was performed by keeping the sample either at 80 K or at 5.2 K. During O_2 dosing, the tip was retracted from the surface by about 10 μm.

3. COMPUTATIONAL DETAILS

All the calculations were performed with the Vienna ab initio simulation package (VASP) with the generalized gradient approximation of Perdew, Burke, and Ernzerhof (PBE-GGA).[32−35] The TiO_2-(110)-1×1 surface was modeled by periodically repeated slabs consisting of a 4 × 2 cell with five O−Ti−O trilayers separated by 15 Å of vacuum. One of the bridge-bonded oxygen atoms in the uppermost layer was removed to mimic the oxygen vacancy. A plane-wave basis set with an energy cutoff of 460 eV and the projector-augmented wave (PAW) potential were employed.[36] Monhkorst-3 Pack grids of 2 × 2 × 1 *K*-points were used. During the optimization, only atoms in the upper two trilayers were allowed to relax until the self-consistent forces were smaller than 0.01 eV/Å. The STM images were simulated by the Tersoff−Hamann formula.[37,38]

4. RESULTS AND DISCUSSION

4.1. Adsorption of Molecular O_2 at BBO_V with a Low Coverage. Parts a and b of Figure 1 give a pair of images for the reduced TiO_2(110)-1×1 surface before and after the exposure of 0.04 langmuir of O_2 (1 langmuir = 1.33 × 10^{-6} mbar·s). Figure 1a shows a typical empty-state STM image of reduced TiO_2(110)-1×1, with alternating rows of 5-fold-coordinated Ti atoms (Ti_{5c}) as bright rows and 2-fold-coordinated bridge-bonded O atoms (BBO) as dark rows. The bright protrusions in the BBO rows are the oxygen vacancies (BBO_V) with a concentration of 0.08 monolayer (1 monolayer = 5.2 × 10^{14} cm^{-2}). It is observed that after O_2 dosing some of the BBO_Vs become almost misty (marked by squares), and four BBO_Vs remain in the frame, as shown in Figure 1b. The two bright protrusions at Ti_{5c} sites (marked by yellow arrows) are attributed to the O adatoms resulting from the dissociative O_2 at BBO_V.[14,20] Parts c−f of Figure 1 correspondingly give the line profiles along marked lines 1−4 in Figure 1a and marked lines 1′−4′ in Figure 1b. The apparent height of BBO_V changes from about 0.30 Å to a value of about 0.13 Å after O_2 dosing. The observation here suggests that the misty BBO_V can be the adsorption of one molecule of O_2. To support this, we calculated the adsorbed configuration and simulated the image of the adsorbed molecular O_2 at BBO_V with a 4 × 2 unit cell including five O−Ti−O trilayers separated by 15 Å of vacuum based on the basis of density functional theory (DFT). Consistent with the previous calculated results,[10,11,39,40] the O_2 molecule adsorbs at BBO_V with the bond axis perpendicular to the BBO row, as shown in Figure 1g. The O−O bond length is 1.44 Å, which is much longer than the bond length of O_2 in the gas phase, suggesting that the molecular O_2 at BBO_V is doubly charged as O_2^{2-}.[10] Figure 1h shows the simulated STM image, which exhibits a faint contrast for the

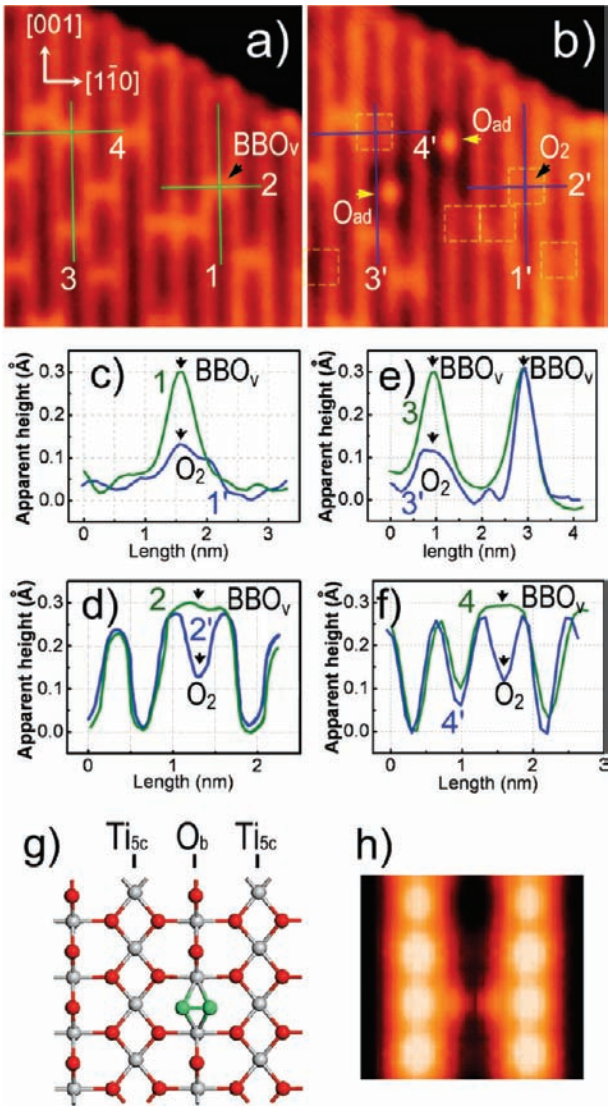

Figure 1. STM images of the hydroxyl-free TiO_2(110)-1×1 surface (a) before and (b) after 0.04 langmuir of O_2 dosing within the same area (size 6.5 × 7.0 nm^2, imaged at 1.0 V and 10 pA, at 80 K). The dashed squares mark the misty BBO_V after O_2 dosing. The yellow arrows mark the O adatoms at Ti_{5c} sites. (c−f) Line profiles giving the relative apparent height change along lines 1−4 marked in (a) and lines 1′−4′ marked in (b), correspondingly. (g) Optimized structure of molecular O_2 adsorbed at BBO_V in top view. (h) Simulated STM image of molecular O_2 adsorbed at BBO_V with a sample bias of 1.0 V (the Fermi level is set to be 0.12 eV below the conduction band minimum) and a constant height of 3.1 Å.

adsorbed O_2 molecule at BBO_V, in good agreement with our experimental observations. Hence, Figure 1b provides the direct image of the singly adsorbed molecular O_2 at BBO_V by comparison in situ with the image in Figure 1a.

4.2. Adsorption of Molecular O_2 with Variable Coverages. Figure 2 shows the results obtained from the stepwise O_2 exposure experiment. In the first step, we allowed the sample to be exposed to 0.02 langmuir of O_2. Figure 2b shows the first scanning frame after exposure of O_2. One can see three misty BBO_Vs, similar to the image in Figure 1b. However, in addition to the misty BBO_Vs, there are some paired protrusions occurring at the neighboring T_{5c} sites in opposite rows of the preexisting

dx.doi.org/10.1021/ja110375n |*J. Am. Chem. Soc.* 2011, 133, 2002–2009

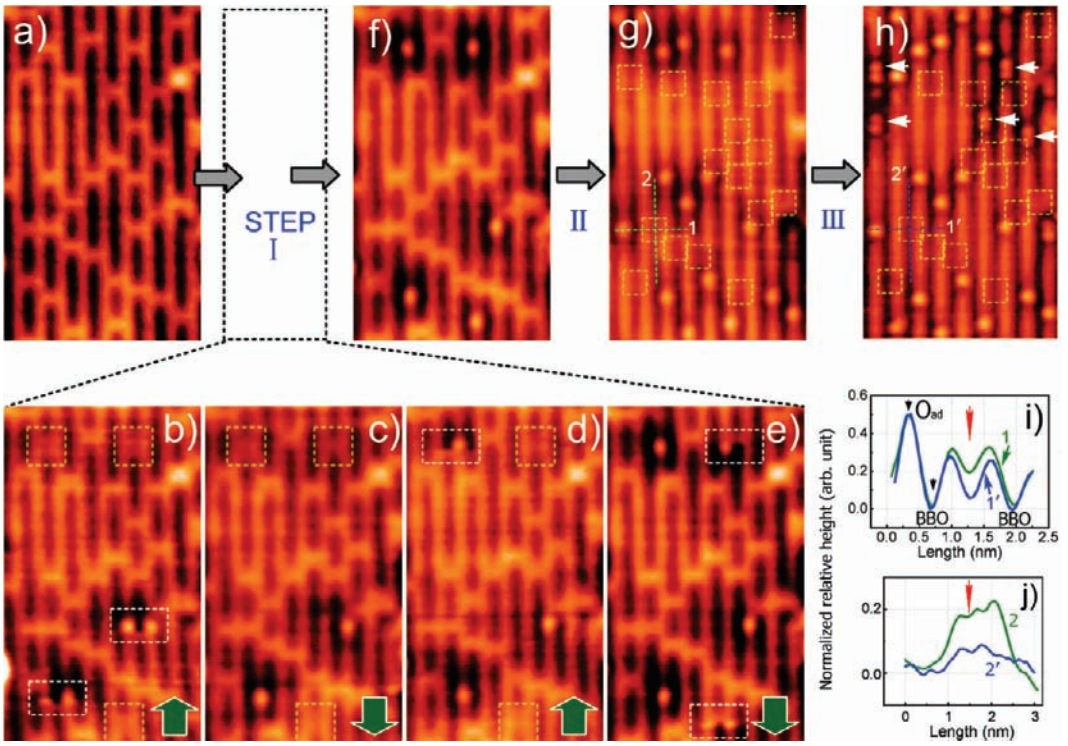

Figure 2. STM images obtained from a stepwise O_2 adsorption process within the same area (size 5.7 × 9.7 nm^2, imaged at 1.0 V and 10 pA, 80 K). (a) Image before O_2 dosing. (b−f) Consecutively acquired images after 0.02 langmuir of O_2 dosing, showing the dissociation of the adsorbed O_2 during scanning (step I). The green arrows show the scanning directions. (g) Image showing the fully filled BBO_V after an additional 0.12 langmuir of O_2 dosing (step II). (h) Image acquired after another additional 0.20 langmuir of O_2 dosing (step III). Dashed squares mark the misty BBO_V with adsorbed molecular O_2, dashed rectangles the intermediate state of the adsorbed molecular O_2 at BBO_V, and white arrows the paired O adatoms presented at Ti_{5c} sites. (i, j) Line profiles corresponding to crossed lines 1 and 2 in (g) and lines 1′ and 2′ in (h). The red arrow denotes the crosspoint of the two lines.

BBO_Vs (marked by rectangles). As we show below, such paired protrusions can be attributed to an intermediate state of an adsorbed O_2 molecule. Hence, there are five adsorbed O_2 molecules in the image. After several cycles of consecutive scanning within the same area at a bias of 1.0 V, all five adsorbed O_2 molecules dissociate and present five O adatoms at the neighboring Ti_{5c} sites (Figure 2b−f). In the second step, we allowed the sample to be further exposed to an additional 0.12 langmuir of O_2, as shown in Figure 2g. It is observed that all of the BBO_Vs are filled by adsorbed O_2, accompanied by some more dissociative O_2 that exhibits as O adatoms at Ti_{5c} sites. In the following step, the sample was exposed to another additional 0.20 langmuir of O_2. Some paired protrusions at the same Ti_{5c} row occur, as marked by the white arrows in Figure 2h. Such types of paired protrusions at the Ti_{5c} row have been observed before,[14] which have been attributed to dissociative O_2 at Ti_{5c}.[7]

It is suggested that two O_2 molecules chemisorb per BBO_V and convert to a stable tetraoxygen as annealed above 200 K, and the tetraoxygen can sustain upon annealing to 400 K.[27,28] As shown in Figure 2g,h, even though the BBO_Vs are fully filled by adsorbed O_2 with excess O_2 dosing, it is difficult to obtain the exact number of adsorbed O_2 molecules per BBO_V from the image. In Figure 2b−f, it is shown that the adsorbed O_2 at a low coverage can be completely dissociated after repeated scanning at 1.0 V within the same area, which can be attributed to the fact that a singly adsorbed O_2 at BBO_V is quite dissociative.[31] However, the image shown in Figure 2h did not follow the same behavior. With repeated scanning at 1.0 V and even at a high bias up to 2.2 V, we observed that the number of O adatoms and the main feature of the surface almost remained unchanged, indicating that the adsorbed O_2 molecules tend to be nondissociative, in contrast to the easily dissociated singly adsorbed O_2 molecules at bias voltages higher than 1.2 V in our experiment. This phenomenon may lead to different explanations. First, one may think that it is due to the total desorption of the adsorbed molecules without dissociation. This argument can be ruled out, since in such a way the preexisting BBO_V should be recovered. Second, the adsorbed O_2 may go through dissociation without leaving an O adatom at such a high coverage, but this is obviously inconsistent with the dissociation behavior of singly adsorbed O_2. A more plausible explanation is that the nondissociative O_2 may contain quite stable oxygen adsorbates with a configuration quite different from that of the singly adsorbed O_2 molecule.

To clarify, a further analysis is made by comparing the relative heights, for example, along the dashed green and blue lines in Figure 2g,h, respectively, as shown in Figure 2i,j. The line profiles have been normalized according to the height difference between the O adatom and the BBO row. It is observed that both profiles of lines 1 and 1′ are almost overlapped, except for the range around the molecular O_2 adsorption site, marked by the red arrow. In this range line 1′ drops to a lower relative height, but not to the same height as the neighboring BBO rows (Figure 2i). Comparison of the line profiles along lines 2 and 2′ shows that both lines also exhibit heights different from those of the other sites in the same BBO row, and line 2 is more protruded than line 2′ around the range marked by the red arrow in Figure 2j. Considering its similarity (lines 1 and 2) to the singly adsorbed molecular O_2 shown above, we suggest that it is a singly adsorbed O_2 molecule

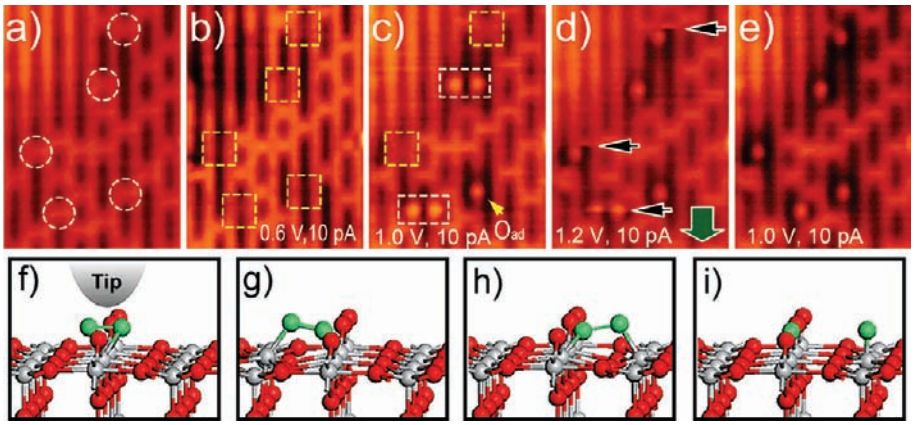

Figure 3. (a) Image of the bare TiO_2(110)-1×1 surface (size 5.2 × 7.2 nm^2, acquired at 1.0 V and 10 pA). Dashed circles mark the original BBO_V sites. (b−e) Images acquired after 0.02 langmuir of O_2 dosing, acquired at different bias voltages. Squares mark BBO_V with adsorbed molecular O_2 and rectangles the intermediate state of the adsorbed O_2. Dark arrows in (d) mark the scratches, and the green arrow denotes the scanning direction. Schematic drawings showing (f) molecular O_2 under the tip at its equilibrium site, (g) molecular O_2 inclined to the left Ti_{5c} site, (g) molecular O_2 inclined to the right Ti_{5c} site, and (i) dissociative O_2.

at the corresponding BBO_V site in Figure 2g. Even though it becomes much dimmer in Figure 2h, the line profiles (line 1′ and 2′) show that it is different from a singly adsorbed molecule, but also different from a bare BBO site. Considering that the total O_2 exposure is about 0.34 langmuir for Figure 2h, doubled compared to the O_2 exposure of 0.14 langmuir for Figure 2g, we tend to believe that the BBO_V should adsorb simultaneously two or more O_2 molecules, which may imply the existence of a stable configuration with more adsorbed molecules per BBO_V, as suggested before.[27,28]

4.3. STM-Tip-Induced Dissociation of Adsorbed Molecular O_2 at BBO_V. The results in the previous STM studies showed dissociative O_2, dominantly with one O atom healing the BBO_V and the other O atom leaving at the neighboring Ti_{5c} site as an adatom.[18,20−22] Here, we observed that the dissociation of O_2 is induced by the STM tip at a low O_2 coverage, in which molecular O_2 singly adsorbs at each BBO_V dominantly. We found that the singly adsorbed O_2 at BBO_V may survive from the tip-induced dissociation when we applied relatively low bias voltages. In Figure 3, we give another set of experimental results. Figure 3b, acquired with a low bias voltage of 0.6 V after the exposure of 0.02 langmuir of O_2, shows a quite similar behavior of adsorbed O_2 at BBO_V. We allowed a repeated scanning in the same area at the bias of 0.6 V. It is observed that the misty BBO_Vs almost remain unchanged at this bias. However, when the bias is increased to about 1.0 V, it is observed that some of the adsorbed O_2 molecules at BBO_V undergo dissociation and produce O adatoms at neighboring Ti_{5c} sites, as shown in Figure 3c. Interestingly, it is also observed that some paired protrusions occur at opposite T_{5c} sites neighboring the adsorbed O_2 at the BBO_V (marked by the rectangles), similar to those in Figure 2b. Such paired protrusions should be an intermediate state of the molecular O_2 before it dissociates. On the basis of our DFT calculations, such an intermediate state can be attributed to the inclined configuration, in good agreement with the theoretical prediction,[39,40] as shown by the schematic drawings in Figure 3f−h. Energetically, the flat-lying configuration in Figure 3f is more preferred than the inclined configuration in Figure 3g (or equivalently in Figure 3h) by about 0.15 eV. The barrier from the flat-lying configuration to the inclined configuration is about 0.5 eV, and the return barrier is small at 0.35 eV.[39] Thus, the paired protrusions are suggested to be a switching behavior between the inclined configuration and the flat-lying equilibrium configuration, which is excited by the inelastic tunneling electron (IETE).[41] With the bias further increased to 1.2 V, the adsorbed O_2 molecules at BBO_V have much higher probability to be dissociated. As shown in Figure 3d, one can see some scratches around the BBO_V with adsorbed O_2 (marked by the dark arrows). The green arrow shows the scanning direction. In principle, the scratches reflect the very fast switching situation of the adsorbed O_2 between the equilibrium state and the intermediate state. At 80 K, once a scratch was observed for the adsorbed O_2 at BBO_V, consequently the O adatoms presented without observation of the intermediate state. This can be rationalized as follows: At a higher bias, the molecularly adsorbed O_2 may have a higher probability to overcome the barrier to the metastable intermediate state with the inclined configuration, caused by the IETE with higher energies when the higher bias voltage is applied. With the inclined configuration, O_2 can be dissociated easily by the IETE with higher energies also, resulting in the dissociation state (Figure 3e and the schematic drawing in Figure 3i). On the basis of the spin-polarized DFT calculations by Chrétien et al.,[40] O_2 dissociation at BBO_V is exothermic by 0.85 eV in the triplet state and the highest barrier is 0.67 eV, and O_2 dissociation is endothermic by 0.11 eV in the singlet state and the barrier is 1.30 eV. According to the dissociation dependence on the bias voltage in our experimental results (see Figure 5), the O_2 dissociation is obviously observed at a voltage of about 0.8 V at 80 K, which suggests most likely that the adsorbed O_2 is in the triplet state and the O_2 dissociation is through the exothermic process.

To confirm the suggestion that the adsorbed O_2 may switch between the different configurations, we measured the tunneling-current (I−t) curve by locating the tip over the adsorbed O_2 molecule. An I−t curve is recorded by locating the STM tip over a specific site and turning off the feedback loop of the STM without scanning. At 80 K, the I−t curve did not give obvious signals showing the switching state. This may be caused by a too fast switching rate to be recorded in the STM images and the I−t curves at 80 K. We then cooled the sample to 5.2 K. Figure 4 shows some representative I−t curves acquired at different bias voltages at 5.2 K. Figure 4a shows the I−t curve acquired at the bias of 1.2 V and the set point current of 10 pA at a misty BBO_V

dx.doi.org/10.1021/ja110375n |J. Am. Chem. Soc. 2011, 133, 2002–2009

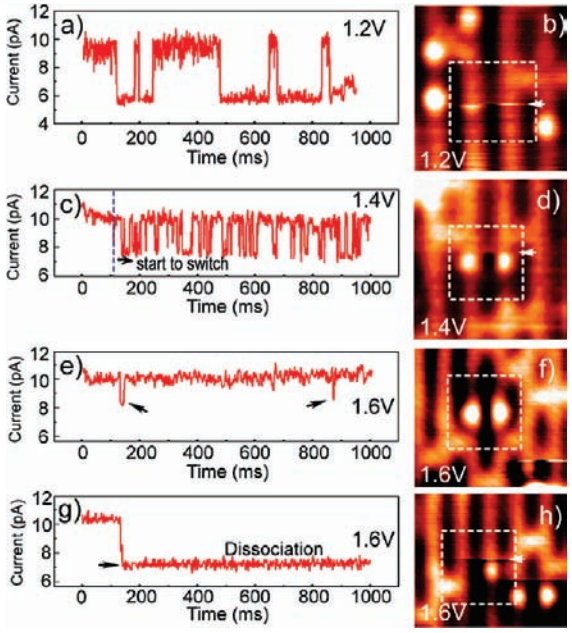

Figure 4. Representive $I-t$ curves and STM images acquired at different bias voltages at 5.2 K: (a, b) at 1.2 V and 10 pA, (c, d) at 1.4 V and 10 pA, (e, f) at 1.6 V and 10 pA, (g, h) at 1.6 V and 10 pA. The $I-t$ curves are acquired at the center of the adsorbed O_2. The images are selected from the large scanning areas correspondingly at the bias voltages and the set point currents indicated. Image sizes: (b) 2.6 × 2.8 nm^2, (d) 2.8 × 3.0 nm^2, (f) 3.4 × 3.1 nm^2, (h) 3.4 × 3.0 nm^2.

with an adsorbed molecule of O_2. The high current state in the $I-t$ curve thus denotes the O_2 molecule under the tip at its equilibrium adsorption site, while the low current state denotes the O_2 molecule off the tip. Correspondingly, we found the behavior of the adsorbed O_2 in the STM images, as shown in Figure 4b. It is noted that as marked by the arrow the bright notches at the two opposite Ti_{5c} rows are not in the same scanning line, reflecting the O_2 either at the left or at the right side of its equilibrium sites. In this case, the adsorbed O_2 molecule mainly stays at its equilibrium site and has a small probability to be excited to either off state as shown in Figure 3g,h. At 1.4 V, the switching rate increases significantly, roughly higher than that at 1.2 V by about 1 order of magnitude, as shown in Figure 4c. In the STM image acquired at 1.4 V (Figure 4d), it becomes difficult to observe a feature similar to that in Figure 4b. At 1.6 V, the feature of the high and the low current states in the $I-t$ curves becomes unobvious, as shown in Figure 4e. According to the results from the low bias voltages, we attribute this phenomenon to the too fast switching rate at 1.6 V. The bandwidth of the preamplifier of the STM instrument used in this experiment is about 800 Hz, so that the signals with higher frequencies than the bandwidth will be cut off. Hence, the $I-t$ curve obtained at 1.6 V reflects the average of the high-frequency signals. At 1.6 V, the adsorbed O_2 has a higher dissociation probability, which has been recorded both in the $I-t$ curves and in the STM images, as shown in Figure 4g,h, respectively. The sudden jump from the high-current state to the low-current state reflects the dissociation of molecular O_2 (Figure 4g). The scratches at opposite Ti_{5c} rows are now in the same scanning line, reflecting the excitation of O_2 and dissociation quickly, as shown in parts f (lower right) and h of Figure 4.

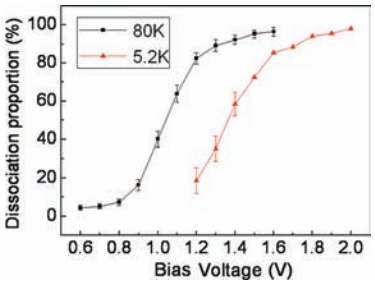

Figure 5. Proportion of dissociated O_2 as a function of the applied bias voltages. The error bars give the standard deviation of the data from more than five runs. The data obtained at higher bias voltages at 5.2 K were simply averaged over just two runs, without giving an error bar.

It thus becomes understandable that the nearly symmetric paired protrusions shown in Figure 3c are caused by the fast switching between the flat-lying equilibrium configuration and the inclined configuration, either on the left or on the right side of the tip, as shown in Figure 3g,h, which are symmetric to the equilibrium state. However, the slow scanning process of the STM instrument can only obtain an average signal of the fast switching states in the images. Similar behavior has been observed in our previous study for another molecular system between two switching states excited by the IETE, which is generally through a multiple-electron process.[41] However, due to the low conductivity of TiO_2, the measurement with a higher tunneling current is difficult. It is currently no possible to decide experimentally whether the IETE-induced dissociation of O_2 is through a multiple-electron process or a single-electron process.

Figure 5 is a plot of the proportion of dissociated O_2 molecules as a function of the applied bias voltage. The proportion of dissociated O_2 is obtained by averaging $\Delta N/N$ at every bias voltage. In each scanning area of the different experimental runs, we counted the number of dissociated O_2 molecules, ΔN. As we have shown above, repeated scanning may induce dissociation of all of the adsorbed molecules even at a not very high bias voltage. To make the data comparable, we counted the number of dissociated O_2 molecules just in the first scanned STM images obtained by using the same scanning speed of 100 nm/s and the same set point current of 10 pA, typically with an area of about 30 × 30 nm^2. The typical O_2 coverage used in such a measurement is about 50% relative to the BBO_V, where the concentration of BBO_V is about 8−12%. The total number of adsorbed O_2 molecules also includes the number of dissociative O_2 molecules. It is observed that at 80 K a distinct increase of the proportion appears when the applied bias voltage is higher than 0.8 V, and almost all of the adsorbed O_2 molecules are dissociated even when scanned only once when the voltage is higher than 1.4 V. This may explain the previous STM observations of only dissociative O_2 since in most cases much higher bias voltages were applied.

4.4. Temperature Dependence of the STM-Tip-Induced O_2 Dissociation. It has been shown that the O_2 adsorption behavior is temperature dependent.[7,8,27] We have further checked the adsorption behaviors of O_2 at various temperatures. For the TiO_2 surface by dosing O_2 at room temperature, we always observed that O_2 is dissociative.[20] Here, we observed that molecular O_2 can be intrinsically adsorbed at BBO_V by O_2 dosing at low temperatures, showing coverage dependence. At 80 K, most of the adsorbed molecular O_2 may survive from the tip-induced dissociation at biases lower than 0.8 V. By warming the sample to a

dx.doi.org/10.1021/ja110375n |J. Am. Chem. Soc. 2011, 133, 2002–2009

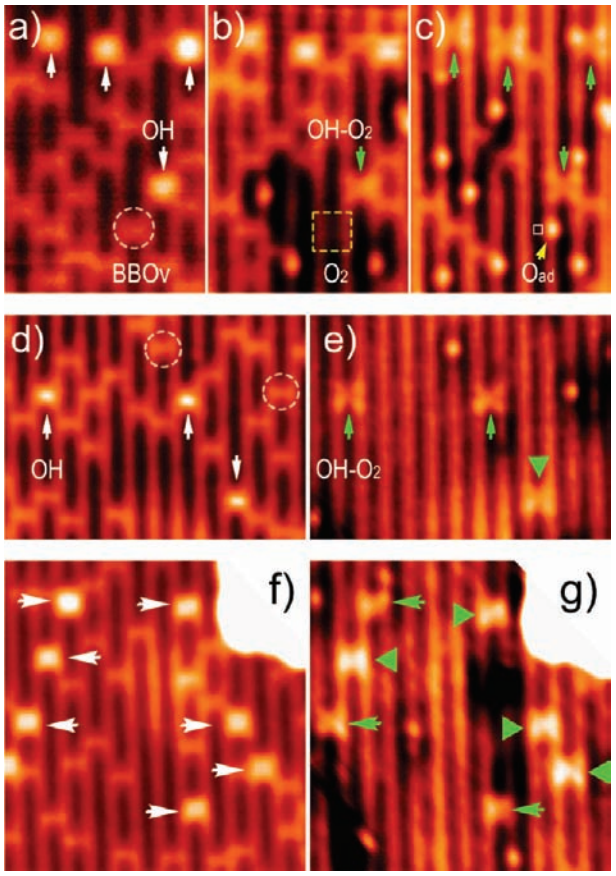

Figure 6. (a) Image of the partially hydroxylated TiO_2(110)-1×1 surface (size 4.5 × 6.5 nm^2, 1.0 V and 10 pA), (b) image acquired after 0.02 langmuir of O_2 dosing, and (c) image acquired after an additional 0.05 langmuir of O_2 dosing. (d, e) Pair of images before and after 0.20 langmuir of O_2 dosing (size 8.1 × 6.0 nm^2, 1.0 V and 10 pA). (f, g) Pair of images before and after 0.30 langmuir of O_2 dosing (size 8.4 × 8.7 nm^2, 1.0 V and 10 pA). Key: white arrows, OH; green arrows, OH−O_2 complex; circles, BBO_V; squares, molecular O_2 at BBO_V.

high temperature of 130 K, we still observed the adsorbed molecular O_2 at BBO_V, but the proportion of dissociated O_2 molecules increased to 20% even at a low bias of 0.6 V. Since it took too long to perform the similar measurement at 130 K, instead, we have performed the measurements at a much lower temperature of 5.2 K. At this temperature, we can only image the surface with a bias higher than 1.2 V and a very low set point current of about 10 pA. The data obtained at 5.2 K are also plotted in Figure 5 for comparison with those obtained at 80 K. At 5.2 K, a similar dependence of O_2 dissociation on the voltage is observed, but for the same value of the proportion, the voltage shifts to a high value by about 0.35 V at 5.2 K. This reflects quite an obvious dissociation dependence on the temperature, in addition to the dependence on the bias voltage.

4.5. Observation of Molecular O_2 Adsorbed at Hydroxyl Sites. The hydroxyl groups have been introduced as another charge donor site to react with O_2 molecules.[15,42,43] The distribution of the excess electrons of OH has been observed to be similar to that of BBO_V, which is delocalized to the neighboring Ti_{5c} sites.[44] To get insight into the electron scavenging process of molecular O_2 on the surface, it is also important to understand the interaction between the molecular oxygen and OH. We prepared the clean TiO_2 sample first and then kept the sample at

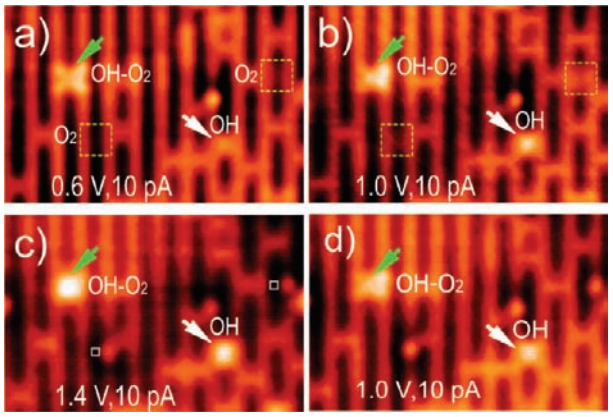

Figure 7. Voltage-dependent images of molecular O_2 adsorbed at OH sites: (a) 0.6 V and 10 pA, (b) 1.0 V and 10 pA, (c) 1.4 V and 10 pA, and (d) 1.0 V and 10 pA after repeated scanning at 1.4 V and 10 pA about 10 times. Size: 7.5 × 4.9 nm^2.

room temperature for about 12 h in a chamber with a base pressure of about 1×10^{-10} mbar before it was transferred to the cryostat of the microscope. In this way, we obtained a partially hydroxylated TiO_2 surface with a few OH groups in the BBO rows, which were produced from the dissociation of background water in the chamber, as shown in Figure 6a. The surface was then exposed to O_2 at 80 K. Parts b and c of Figure 6 show the images obtained from the O_2-dosed sample in two steps. In the first step, we allowed the surface to be exposed to 0.02 langmuir of O_2. Some adsorbed molecular O_2 and dissociative O_2 are also observed, similar to our discussion above. Interestingly, it is observed that one of the OH groups changes from a round shape to an X-like shape, as marked by the green arrow in Figure 6b, while the other three OH groups in the upper panel remain unchanged. In the second step, we allowed the surface to be exposed to an additional 0.05 langmuir of O_2. The other three remaining OH groups now also change from the round shape to the X-like shape (Figure 6c). The shape change of the OH groups here thus can be directly attributed to the adsorption of, most likely, one O_2 molecule at each OH, forming a OH−O_2 complex. Generally, such a OH−O_2 complex shows an asymmetric X-like shape at 1.0 V. Similar behaviors have been observed for the 0.2 langmuir of O_2 dosed sample, as shown in Figure 6d,e. In Figure 6e, all of the BBO_Vs are filled with molecular O_2. It is noted that one of the complexes of O_2 at OH is different from the other two, showing a more protruded and symmetric shape (marked by the triangle). In the sample with a higher exposure of 0.3 langmuir of O_2, more complexes with such a shape present, as shown in Figure 6f,g. The complexes with the more protruded and symmetric shape may be due to the OH containing two or more O_2 molecules. The exact configuration with high coverage of O_2 adsorbed at OH needs further study.

Here we just discuss OH with only one adsorbed O_2 molecule. In our previous work, we have shown that OH exhibits a dependence on the bias voltage and the tunneling current in the STM images.[19] A set of STM images acquired at different bias voltages are given in Figure 7. At a low bias voltage of 0.6 V the OH−O_2 complex shows a relatively symmetric X-like shape (Figure 7a). As a comparison, one can see that OH is just slightly more protruded than BBO_V. At an intermediate bias voltage of 1.0 V the OH−O_2 complex exhibits a asymmetric X-like shape (Figure 7b), and at a high bias voltage of 1.4 V the complex

dx.doi.org/10.1021/ja110375n |J. Am. Chem. Soc. 2011, 133, 2002–2009

becomes a very round shape, similar to the protrusion of the OH in the same frame. To confirm that the round-shaped protrusion of the complex is not due to the desorption of O_2 from the complex, we acquired the image back to a low bias voltage of 1.0 V and found that the X-like shape remains, as shown in Figure 7d. At a higher bias voltage of around 2.2 V, we did not observe desorption of O_2 from the complex. The observation here suggests that the adsorbed molecular O_2 at OH is more stable than that at BBO_V against the IETE. Henderson et al. reported that the O_2 + OH reaction does not occur at low temperatures below 120 K.[45] It is suggested that OH reacts with O_2 at room temperature, yielding an intermediate hydroperoxyl (HO_2) species at the Ti_{5c} site.[9,24] It is observed that the HO_2 species presents as a protrusion at a Ti_{5c} site. However, in our observation the OH−O_2 complex exhibited at a BBO site shows a dependence quite similar to that of OH on the bias voltage, suggesting that the electronic states of the OH in the complex almost remain as the individual OH. This is consistent with results that O_2 and OH do not react at 80 K. The OH−O_2 complex at 80 K could be a precursor of the HO_2 species.

During the manuscript preparation, we noticed some similar works by other groups.[46,47] Scheiber et al.[46] reported the observation of an elusive adsorbate on the O_2-dosed TiO_2 surface, which is assigned to the adsorption of molecular O_2. This is consistent with the misty BBO_V of singly adsorbed molecular O_2 in our observations (Figures 1 and 2). However, we have an explanation for the O_2 dissociation mechanism quite different from their interpretation. Our results strongly suggest the dissociation of O_2 undergoes an intermediate state, as discussed above, illustrated in Figure 3f−h, and evidenced by the switching behavior as shown in Figure 4. Moreover, our results show that molecular O_2 adsorbed at OH can be very stable and also indicate the existence of stable O_2 adsorbates with the BBO_V fully filled surface by excess O_2 dosing, different from the dissociative behavior of singly adsorbed O_2 at BBO_V. A more recent work by Wang et al.[47] reported that molecular O_2 can adsorb both at BBO_V and at Ti_{5c} sites. They found that molecular O_2 can be observed at Ti_{5c} sites with rather extremely low parameters of the bias voltage and the tunneling current of 0.3 V and 1 pA, respectively, whereas O_2 molecules at Ti_{5c} sites become dissociative at 0.6 V and 1pA, suggesting a quite easy STM-tip-induced O_2 dissociation process. This may explain our observation of only dissociative O_2 at Ti_{5c} sites since we typically imaged the surface at biases higher than 0.6 V.

5. CONCLUSIONS

In conclusion, we have systematically studied the adsorption behaviors of molecular O_2 at BBO_V on the reduced TiO_2(110)-1×1 surface using low-temperature STM. We provide direct evidence that molecular O_2 intrinsically adsorbs at the defect sites of BBO_V and OH of the surface by comparing the performance of the adsorbed O_2. The adsorbed molecular O_2 at BBO_V can be dissociated by the IETEs from the STM tip under relatively high bias voltages. The tip-induced dissociation of O_2 undergoes an intermediate state in which the molecular O_2 is excited from its flat-lying equilibrium adsorption site, centered at BBO_V, to an offset site with an inclined configuration by the IETE. The tip-induced dissociation also shows the dependence on the applied bias voltage and the temperature. Differently, singly adsorbed molecular O_2 at OH can survive from the tip-induced dissociation under relatively high bias voltages, showing that the adsorbed O_2 at OH is more stable than that at BBO_V. Our findings here provide useful and important information for the atomic-scale study of O_2-related chemical processes.

AUTHOR INFORMATION

Corresponding Author
bwang@ustc.edu.cn; jghou@ustc.edu.cn

ACKNOWLEDGMENT

We appreciate the helpful discussion with Prof. Jin Zhao and Prof. Yi Luo. This work was supported by the NBRP (Grant 2011CB921400) and NSFC (Grants 50721091, 90921013, 10825415, 60771006, and 20873129), China.

REFERENCES

(1) Dohnálek, Z.; Lyubinetsky, I.; Rousseau, R. *Prog. Surf. Sci.* **2010**, *85*, 161.
(2) Diebold, U. *Surf. Sci. Rep.* **2003**, *48*, 53.
(3) Diebold, U.; Lehman, J.; Mahmoud, T.; Kuhn, M.; Leonardelli, G.; Hebenstreit, W.; Schmid, M.; Varga, P. *Surf. Sci.* **1998**, *411*, 137.
(4) Haruta, M.; Kobayashi, T.; Sano, H.; Yamada, N. *Chem. Lett.* **1987**, *2*, 405.
(5) Thompson, T. L.; Yates, J. T. *Chem. Rev.* **2006**, *106*, 4428.
(6) Lu, G. Q.; Linsebigler, A.; Yates, J. T. *J. Chem. Phys.* **1995**, *102*, 4657.
(7) Wendt, S.; Sprunger, P. T.; Lira, E.; Madsen, G. K. H.; Li, Z. S.; Hansen, J. Ø.; Matthiesen, J.; Blekinge-Rasmussen, A.; Lægsgaard, E.; Hammer, B.; Besenbacher, F. *Science* **2008**, *320*, 1755.
(8) Henderson, M. A.; Epling, W. S.; Perkins, C. L.; Peden, C. H. F.; Diebold, U. *J. Phys. Chem. B* **1999**, *103*, 5328.
(9) Papageorgiou, A. C.; Beglitis, N. S.; Pang, C. L.; Teobaldi, G.; Cabailh, G.; Chen, Q.; Fisher, A. J.; Hofer, W. A.; Thornton, G. *Proc. Natl. Acad. Sci. U.S.A.* **2010**, *107*, 2391.
(10) Tilocca, A.; Selloni, A. *ChemPhysChem* **2005**, *6*, 1911.
(11) Rasmussen, M. D.; Molina, L. M.; Hammer, B. *J. Chem. Phy.* **2004**, *120*, 988.
(12) Lira, E.; Hansen, J. Ø.; Huo, P.; Bechstein, R.; Galliker, P.; Lægsgaard, E.; Hammer, B.; Wendt, S.; Besenbacher, F. *Surf. Sci.* **2010**, *604*, 1945.
(13) Pang, C. L.; Lindsay, R.; Thornton, G. *Chem. Soc. Rev.* **2008**, *37*, 2328.
(14) Cui, X. F.; Wang, B.; Wang, Z.; Huang, T.; Zhao, Y.; Yang, J. L.; Hou, J. G. *J. Chem. Phys.* **2008**, *129*, 044703.
(15) Deskins, N. A.; Rousseau, R.; Dupuis, M. *J. Phys. Chem. C* **2010**, *114*, 5891.
(16) Du, Y. G.; Deskins, N. A.; Zhang, Z. R.; Dohnalek, Z.; Dupuis, M.; Lyubinetsky, I. *Phys. Chem. Chem. Phys.* **2010**, *12*, 6337.
(17) Epling, W. S.; Peden, C. H. F.; Henderson, M. A.; Diebold, U. *Surf. Sci.* **1998**, *412*−*13*, 333.
(18) Wendt, S.; Schaub, R.; Matthiesen, J.; Vestergaard, E. K.; Wahlström, E.; Rasmussen, M. D.; Thostrup, P.; Molina, L. M.; Lægsgaard, E.; Stensgaard, I.; Hammer, B.; Besenbacher, F. *Surf. Sci.* **2005**, *598*, 226.
(19) Cui, X. F.; Wang, Z.; Tan, S. J.; Wang, B.; Yang, J. L.; Hou, J. G. *J. Phys. Chem. C* **2009**, *113*, 13204.
(20) Wang, Z.; Zhao, Y.; Cui, X.; Tan, S.; Zhao, A.; Wang, B.; Yang, J.; Hou, J. G. *J. Phys. Chem. C* **2010**, *114*, 18222.
(21) Bikondoa, O.; Pang, C. L.; Ithnin, R.; Muryn, C. A.; Onishi, H.; Thornton, G. *Nat. Mater.* **2006**, *5*, 189.
(22) Du, Y. G.; Dohnálek, Z.; Lyubinetsky, I. *J. Phys. Chem. C* **2008**, *112*, 2649.
(23) Zhang, Z.; Lee, J.; Yates, J. T.; Bechstein, R.; Lira, E.; Hansen, J. Ø.; Wendt, S.; Besenbacher, F. *J. Phys. Chem. C* **2010**, *114*, 3059.

(24) Du, Y. G.; Deskins, N. A.; Zhang, Z. R.; Dohnálek, Z.; Dupuis, M.; Lyubinetsky, I. *J. Phys. Chem. C* **2009**, *113*, 666.
(25) Matthiesen, J.; Wendt, S.; Hansen, J. Ø.; Madsen, G. K. H.; Lira, E.; Galliker, P.; Vestergaard, E. K.; Schaub, R.; Lægsgaard, E.; Hammer, B.; Besenbacher, F. *ACS Nano* **2009**, *3*, 517.
(26) Zhang, Z.; Du, Y.; Petrik, N. G.; Kimmel, G. A.; Lyubinetsky, I.; Dohnálek, Z. *J. Phys. Chem. C* **2009**, *113*, 1908.
(27) Kimmel, G. A.; Petrik, N. G. *Phys. Rev. Lett.* **2008**, *100*, 196102.
(28) Pillay, D.; Wang, Y.; Hwang, G. S. *J. Am. Chem. Soc.* **2006**, *128*, 14000.
(29) Linsebigler, A. L.; Lu, G. Q.; Yates, J. T. *Chem. Rev.* **1995**, *95*, 735.
(30) Fujishima, A.; Zhang, X. T.; Tryk, D. A. *Surf. Sci. Rep.* **2008**, *63*, 515.
(31) Petrik, N. G.; Kimmel, G. A. *J. Phys. Chem. Lett.* **2010**, *1*, 1758.
(32) Kresse, G.; Hafner, J. *Phys. Rev. B* **1993**, *48*, 13115.
(33) Kresse, G.; Hafner, J. *Phys. Rev. B* **1993**, *47*, 558.
(34) Kresse, G.; Hafner, J. *Phys. Rev. B* **1994**, *49*, 14251.
(35) Kresse, G.; Joubert, D. *Phys. Rev. B* **1999**, *59*, 1758.
(36) Lindan, P. J. D.; Harrison, N. M.; Gillan, M. J.; White, J. A. *Phys. Rev. B* **1997**, *55*, 15919.
(37) Tersoff, J.; Hamann, D. R. *Phys. Rev. Lett.* **1983**, *50*, 1998.
(38) Tersoff, J.; Hamann, D. R. *Phys. Rev. B* **1985**, *31*, 805.
(39) Wang, Y.; Pillay, D.; Hwang, G. S. *Phys. Rev. B* **2004**, *70*, 193410.
(40) Chrétien, S.; Metiu, H. *J. Chem. Phys.* **2008**, *129*, 074705.
(41) Pan, S. A.; Fu, Q.; Huang, T.; Zhao, A. D.; Wang, B.; Luo, Y.; Yang, J. L.; Hou, J. G. *Proc. Natl. Acad. Sci. U.S.A.* **2009**, *106*, 15259.
(42) Liu, L. M.; Crawford, P.; Hu, P. *Prog. Surf. Sci.* **2009**, *84*, 155.
(43) Petrik, N. G.; Zhang, Z. R.; Du, Y. G.; Dohnalek, Z.; Lyubinetsky, I.; Kimmel, G. A. *J. Phys. Chem. C* **2009**, *113*, 12407.
(44) Minato, T.; Sainoo, Y.; Kim, Y.; Kato, H. S.; Aika, K.; Kawai, M.; Zhao, J.; Petek, H.; Huang, T.; He, W.; Wang, B.; Wang, Z.; Zhao, Y.; Yang, J. L.; Hou, J. G. *J. Chem. Phys.* **2009**, *130*, 124502.
(45) Henderson, M. A.; Epling, W. S.; Peden, C. H. F.; Perkins, C. L. *J. Phys. Chem. B* **2003**, *107*, 534.
(46) Scheiber, P.; Riss, A.; Schmid, M.; Varga, P.; Diebold, U. *Phys. Rev. Lett.* **2010**, *105*, 216101.
(47) Wang, Z.-T.; Du, Y.; Dohnálek, Z.; Lyubinetsky, I. *J. Phys. Chem. Lett.* **2010**, *1*, 3524.